# Detection of Copy Number Alterations in Metastatic Melanoma by a DNA Fluorescence *In situ* Hybridization Probe Panel and Array Comparative Genomic Hybridization: A Southwest Oncology Group Study (S9431)

Stephen R. Moore,[1] Diane L. Persons,[2] Jeffrey A. Sosman,[3] Dolores Bobadilla,[1] Victoria Bedell,[1] David D. Smith,[1] Sandra R. Wolman,[4] Ralph J. Tuthill,[5] Jim Moon,[6] Vernon K. Sondak,[7] and Marilyn L. Slovak[1]

**Abstract**

**Purpose:** Gene copy number alteration (CNA) is common in malignant melanoma and is associated with tumor development and progression. The concordance between molecular cytogenetic techniques used to determine CNA has not been evaluated on a large set of loci in malignant melanoma.

**Experimental Design:** A panel of 16 locus-specific fluorescence *in situ* hybridization (FISH) probes located on eight chromosomes was used to identify CNA in touch preparations of frozen tissue samples from 19 patients with metastatic melanoma (SWOG-9431). A subset ($n = 11$) was analyzed using bacterial artificial chromosome (BAC) array comparative genomic hybridization (aCGH) of DNA isolated directly from touch-preparation slides.

**Results:** By FISH, most samples showed loss near or at *WISP3*/6p21, *CCND3*/6q22, and *CDKN2A*/9p21 (>75% of samples tested). More than one third of *CDKN2A*/9p21 losses were biallelic. Gains of *NEDD9*/6p24, *MET*/7q31, and *MYC*/8q24 were common (57%, 47%, and 41%, respectively) and CNA events involving 9p21/7p12.3 and *MET* were frequently coincident, suggesting gain of the whole chromosome 7. Changes were confirmed by aCGH, which also uncovered many discreet regions of change, larger than a single BAC. Overlapping segments observed in >45% of samples included many of the loci analyzed in the FISH study, in addition to other WNT pathway members, and genes associated with TP53 pathways and DNA damage response, repair, and stability.

**Conclusions:** This study outlines a set of CNAs at the gene and regional level, using FISH and aCGH, which may provide a benchmark for future studies and may be important in selection of individual therapy for patients with metastatic malignant melanoma.

Skin cancer occurs in more than 1,200,000 Americans annually (1). Most cases are highly curable squamous and basal cell cancers, but ~62,500 new cases of melanoma will be diagnosed this year in the United States. The incidence of melanoma has steadily been increasing, and melanoma causes more than 8,400 deaths per year in this country, accounting for the vast majority of skin cancer deaths (1). Early detection and surgery are key to improved survival. Once metastatic melanoma is diagnosed, median survival duration of only 6 to 9 months is expected.

Primary melanoma lesions have largely been characterized by Breslow's depth, Clark's level, ulceration, microscopic involvement of regional lymph nodes, as well as mitotic index, lymphocyte infiltration, and signs of regression. Metastatic melanoma is staged based on location of lesions, such as skin, lymph nodes, lung, liver, and other organ sites, and finally, serum lactate dehydrogenase. With advances in genetic technology, new tools have been developed that may facilitate the collection of a set of potentially robust prognostic genetic indicators (2, 3) to augment the anatomic classifications.

Cytogenetic, molecular, and biological studies indicate that multiple genetic alterations are involved in the development and progression of malignant melanoma, with several genes and chromosomal sites deleted, amplified, overexpressed, or silenced, many of which are detectable at the chromosomal level (3). Fluorescence *in situ* hybridization (FISH) has been

**Authors' Affiliations:** [1]City of Hope, Duarte, California; [2]University of Kansas Medical Center, Kansas City, Kansas; [3]Vanderbilt University School of Medicine, Nashville, Tennessee; [4]George Washington University School of Medicine, Washington, District of Columbia; [5]Cleveland Clinic Foundation, Cleveland, Ohio; [6]Southwest Oncology Group Statistical Center, Seattle, Washington; and [7]H. Lee Moffitt Cancer Center, University of South Florida, Tampa, Florida

Received 8/30/07; revised 1/30/08; accepted 1/31/08.

**Grant support:** Public Health Service Cooperative Agreement grants CA38926, CA32102, CA46368, CA04919, and CA73590 awarded by the National Cancer Institute, Department of Health and Human Services.

The costs of publication of this article were defrayed in part by the payment of page charges. This article must therefore be hereby marked *advertisement* in accordance with 18 U.S.C. Section 1734 solely to indicate this fact.

**Requests for reprints:** Marilyn L. Slovak, City of Hope, Department of Cytogenetics, Northwest Building, Room 2255, 1500 East Duarte Road, Duarte, CA 91010. Phone: 626-256-4673, ext. 62313; Fax: 626-301-8877; E-mail: mslovak@coh.org.



doi:10.1158/1078-0432.CCR-07-4068

used extensively, especially when sample size is limited, to evaluate individual chromosome imbalance, or copy number alteration (CNA) associated with metastatic progression (4), and to classify CNA related to anatomic site (5). Some of the genes identified include members of the receptor tyrosine kinase family (*FGFR3*, *EGFR*), oncogenes (*KIT*, *MET*, *MYC*), genes involved in development (*MITF*, *WNT5A*), and genes involved in regulation of cell cycle progression (*CDKN2A*) and apoptosis (*APAF1*). More recently, array comparative genomic hybridization (aCGH) has emerged as a relatively high-resolution (~30× conventional cytogenetics) tool with which to assess CNA across the genome in a single assay. Unlike FISH, aCGH does not require that a gene of interest be targeted, and aCGH can detect CNA events involving genomic regions as large as whole chromosomes, aberrations that have been reported frequently for melanoma using conventional cytogenetics (6) or aCGH (7, 8). The aCGH data processing and segmentation algorithm permits the conversion of intensity ratios into discrete segments of change easily visible within the processing platforms. The result of this segmentation is a reduction of resolution of aCGH to two to three elements [e.g., bacterial artificial chromosomes (BAC)]. Individual BACs are often used as FISH probes to support aCGH findings (9).

In this study, we used a collection of locus-specific FISH probes and aCGH to determine copy number in a set of genes presumed to be important in the etiology of malignant melanoma, using touch preparations from frozen tissue samples collected from patients registered on the Southwest Oncology Group protocol S9431.

## Materials and Methods

### Patient samples

Samples were obtained from patients registered on S9431. Patients were enrolled before undergoing resection of their metastatic disease with the intent to remove all gross disease. Of the 19 patients enrolled, all were White/non-Hispanic except one, who was Black/non-Hispanic. These patients generally had isolated metastases with only one to five lesions and were defined as having disease beyond regional lymph nodes. Tissue (>5 $mm^3$) collected at biopsy/surgery was snap frozen immediately after resection at -150°C in isopentane-quenched liquid nitrogen and submitted to the University of Cincinnati Tumor Tissue Bank (Cincinnati, OH) where it remained frozen until use. Tissue samples containing metastatic melanoma from 19 patients were collected and considered sufficient and evaluable for further study.

### Sample preparation

Touch preparations were made from tissue samples obtained from frozen-banked material from the University of Cincinnati Tumor Tissue Bank. A cut surface was made on each frozen tissue sample with a scalpel and the surface gently touched to a clean glass microscope slide. Slides were immediately placed in Carnoy's fixative (3:1 methanol/acetic acid) for 30 min, then allowed to air dry. Slides were stored at -20°C until hybridization was done.

### FISH

***Probe selection.*** For this study, a panel of 16 locus-specific FISH probes located on eight chromosomes was used (Table 1). FISH probes were chosen based on previous reports implicating their potential role in the development or progression of malignant melanoma (references in Table 1). All RPCI-11 clones used were obtained from Dr. Pieter J. de Jong (Children's Hospital Oakland Research Institute, Oakland, CA). The probe targeting *FGFR3* was a gift from Dr. Mariano Rocchi (University of Bari, Bari, Italy). Jefferson Medical College (Philadelphia, PA) provided the probe targeting *MYC*. The probe targeting *CDKN2A* was a gift from Dr. Alexander Kamb (Myriad Genetics, Inc., Salt Lake City, UT). California Institute of Technology (Pasadena, CA) provided the probes targeting *KIT*, *EGFR*, and *MET*. The DNA probes developed for the melanoma testing panel included *MITF* (3p44), *WNT5A* (3p21), *FGFR3* (4p12), *KIT* (4q12), *NEDD9* (6p24.1), *CCND3* (6p21), *WISP3* (6q22), *EGFR* (7p12.3), *MET* (7q31), *MYC* (8q24), *MLANA* (9p24.1), *CDKN2A* (9p21), *CD82* (11p11.2), *NCAM1* (11q23), *ETS1* (11q24), and *APAF1* (12q23). Each test probe was paired with a reference probe in either the opposite chromosome arm or the chromosome centromere to control for numerical or ploidy changes. This strategy was complicated by the fact that in some cases [e.g., *WISP3* (6q) and *CCND3* (6p) or *NEDD9* (6p)], losses of 6q and gains of 6p were coincident. For this reason, we based our classification of gain or loss on the ploidy of the sample as determined by the Feulgen method (below).

***Probe preparation, hybridization, and microscopic analysis.*** DNA was isolated from BAC clones using standard methods and labeled by nick translation according to the manufacturer's recommendations (Abbott Molecular, Inc.). Probe (100 ng) was denatured, applied to fresh touch-preparation microscope slides, and the slides were hybridized in a 37°C humidified chamber overnight. Posthybridization washes were done as follows: 50% formamide/2× SSC wash at 45°C for 15 min with agitation every 5 min, 2× SSC wash at 37°C for 8 min, and 1× PBD wash at room temperature for 2 min. Slides were mounted using Vectashield mounting medium with 4′,6-diamidino-2-phenylindole (Vector Laboratories). Probes were validated before use on patient sample material by (*a*) mapping to previously defined normal cellular loci using normal human lymphocyte metaphases and (*b*) testing for hybridization efficiency and robustness in interphase cells (fresh and frozen; data not shown). Coded FISH slides were scored using a Nikon microscope equipped with 4′,6-diamidino-2-phenylindole/FITC/Texas red triple filter and FITC and Rhodamine single bandpass filters. Between 50 and 200 nuclei per probe set were scored by two independent researchers for all targets (mean ± SE, 59 ± 3.84; range, 24-200). Some rare cases were included where <50 evaluable cells were available for scoring, but these represented <10% of the total and composed at least 20 cells (mean ± SE, 36.3 ± 2.67; range, 24-49) in each case.

***Classification of probe gains and losses.*** The following guidelines were used for classification of FISH signal patterns as probe gains or losses: (*a*) each sample must have at least 20 scorable cells (≥90% of samples had >50 scorable cells for each probe) and (*b*) aberrant signal patterns must constitute at least 30% of the analyzed cell population to be scored as a gain or loss. Due to a concern about coincident gain or loss of paired probes (see above), gains or losses were assessed independently for each probe combination by comparing signal number to DNA content (below).

***DNA content (ploidy) determination.*** Specimens were stained by the Feulgen method using the CAS DNA staining kit (Cell Analysis System, Becton Dickinson) according to the manufacturer's instructions. Feulgen-stained rat hepatocytes served as control cells. Slides were evaluated by a CAS-200 image analyzer (Becton Dickinson) with Quantitative DNA Analysis Software (QDA). The DNA content of a minimum of 200 nuclei was measured and classified as diploid (DNA index, 0.8-1.2), tetraploid (DNA index, 1.8-2.2), or aneuploid (DNA index, >1.2, <1.8, or >2.2).

### aCGH

***Isolation and amplification of DNA from touch preparations.*** Cells were manually isolated from microscope slides using a sterile surgical scalpel essentially as described by Nowak et al. (9). However, in the current study, no effort was made to discriminate or isolate particular fractions of cells. All of the cells on the slide were used for isolation of DNA, amplification, and subsequent aCGH, which we felt would facilitate a more linear comparison with the FISH study, in which all of the cells on the slide were probed and examined. DNA was extracted

following the manufacturer's protocol (Qiagen EZ1 DNA Extraction Kit, Qiagen, Inc.) and was amplified to yield sufficient DNA for aCGH using random fragmentation whole genome amplification following the manufacturer's instructions (WGA2, Sigma-Aldrich). Quantity and quality of amplified DNA were highly reproducible, as was recently reported for this technique (9).

***aCGH analysis.*** Reference and test DNA (1 μg each) were fluorescently labeled using the Enzo BioArray CGH Labeling System (Enzo Biochem, Inc.). DNA was combined and used for hybridization to the RPCI 19k BAC array as described (10). The hybridized slides were scanned (GenePix 4200AL Scanner, Molecular Devices Corp., MDS, Inc.) and the resulting high-resolution (5 μm) images [one for control (Cy3) and one for test (Cy5)] were imported into the Imagene version 7.5 aCGH analysis program (Biodiscovery, Inc.).

***Statistical analysis.*** The ratio (tumor/control) of fluorescence intensity was converted on a log 2 scale. Data points (log 2 ratio for each BAC) were segmented across the genome using a rank segmentation algorithm that incorporates circular binary segmentation (11) to define regions of CNA. The significance threshold for segmentation was conservative ($P = 0.001$), minimizing the detection of false positives. An arbitrary threshold for detection of copy number gains and losses was set at 50% of the population with a copy number gain or loss, which corresponds to a log 2 ratio value of 0.319 or -0.192, respectively. This 50% threshold was more conservative than the 30% requirement for the FISH data in consideration of the natural variation in aCGH data.

***General trends of CNA across samples.*** Data from Imagene were imported into Nexus version 8.0 software program (Biodiscovery) to build an aggregate aCGH profile based on the frequency of a particular CNA segment in the population of samples. Data are not pooled for individual BACs, nor is circular binary segmentation done on the larger data set; rather, each segment in each sample is considered independently in the context of the overall mean and variation of that sample, just as in Imagene, and the frequency that any particular segment is ranked as a gain or loss is used to build the aggregate. The Nexus program also facilitated the identification of minimal regions of CNA that were similar across samples, and only those segments that were observed in 3 or more of the 11 (27%) samples were reported in the

**Table 1.** DNA FISH probes used

| Target gene (band) | Function | Clone; distance to target (control locus, band, clone) | Reference |
|---|---|---|---|
| *MITF* (3p14.1) | Melanocyte differentiation and development. "Lineage-specific oncogene" in malignant melanoma; transcriptional regulator of many melanoma-associated proteins, BCL2 and MLANA. | RP11-154H23; 1.5 Mb centromeric to MIT (*MLF1, 3q25, RP112193B07*) | (3, 31–33) |
| *WNT5A* (3p21.2) | Overexpressed message, directly affects cell motility and invasion in melanoma; associated with tumor grade. Involved in β-catenin activation. | RP11-169G24; 0.67 Mb centromeric to *WNT5A* (*MLF1 3q25, RP112193B07*) | (34) |
| *FGFR3* (4p16) | Receptor tyrosine kinase; inhibition can prevent tumor growth. | DJ1054L13 (*KIT*) | (35) |
| *KIT* (4q12) | *KIT* oncogene, amplified in malignant melanoma. Mast cell growth factor receptor. Stem cell factor receptor. | AQ562774; 0.046 Mb centromeric to *KIT* (*FGFR3*) | (36) |
| *CCND3* (6p21) | Up-regulated in melanoma cells. High levels associated with early relapse and decreased survival for superficial (not nodular) melanoma. | RP11-3060I3 (*WISP3*) | (37, 38) |
| *NEDD9* (6p24.1) | Melanoma metastasis gene, frequently amplified, 6p gains common in metastatic melanoma. | RP11-679B17; 0.3 MB centromeric to *NEDD9* (*WISP3*) | (23) |
| *WISP3* (6q22) | Loss correlates with overexpression of RhoC GTPase, essential for metastasis/tumor cell invasion. | RP11-28L24; 0.01 Mb centromeric to *WISP3* (*CCND3* or *NEDD9*) | (39–41) |
| *EGFR* (7p12.3-p12.1) | Tyrosine kinase receptor; activates MAPK/ERK. Involved in β-catenin activation. Trisomy 7 and *EGFR* amplification common in melanoma. | CTD-2026N22; 0.0 Mb from EGFR (*MET*) | (42) |
| *MET* (7q31) | Proto-oncogene, key regulator of invasive growth. | AC004416; 0.0 Mb from *MET* (*EGFR*) | (43) |
| *MYC* (8q24) | Transcription of growth-related genes. *MYC* amplification and *CDKN2A* loss in nodular melanoma associated with improved survival. | I2, P72 (*8cen, PZ8.4*) | (44) |
| *MLANA* (9p24.1) (*MART-1*) | Melanin synthesis, marker of melanocytic differentiation. Human melanoma antigen recognized by T cells. Possible role in progression. | RP11-147N16 (*ABL, 9q34, 1132H12, 835J22*) | (45, 46) |
| *CDKN2A* (9p21) | Gene products INK4A/p16 and ARF —S-phase progression and MDM2 regulation, respectively. Deletions and mutations in 9p12 common in primary melanoma. Familial melanoma. | P1 1069 (*ABL, 9q34, 1132H12, 835J22*) | (19–21) |
| *CD82* (11p11.2) | Deletion (LOH) or loss of expression. Tumor metastasis suppressor gene activated by p53. | RP11-222G13 (*NCAM1*) | (26, 47) |
| *NCAM1* (11q23) | Down-regulated in association with loss of 11q23. Disruption may lead to invasion and metastasis. | RP11-47N15; 0.54 Mb centromeric to *NCAM1* (*CD82*) | (48) |
| *ETS1* (11q24) | Transcriptional regulator of BMP4, associated with metastasis. Widely expressed in melanocytes. | RP11-20M1; 2.0 Mb from *ETS1* (*CD82*) | (49, 50) |
| *APAF1* (12q23) | Important player in mitochondrial mediated apoptosis. Decreased expression associated with disease progression. LOH at 12q23 associated with poor prognosis. | RP11-210L7; 3.66 Mb from *APAF1* (*12cen, PBR12*) | (51, 52) |

Abbreviations: MAPK, mitogen-activated protein kinase; ERK, extracellular signal–regulated kinase; MDM, murine double minute 2; LOH, loss of heterozygosity.

current study. Nexus integrates the recently published normal copy number variation (CNV) database (12) for reference comparisons.

***Statistical comparison of FISH data to aCGH data.*** We assessed aCGH log 2 ratio values at the precise BACs that were used in the FISH study. The log 2 ratio values were bracketed either by 1 SD or by a log 2 ratio value representing 30% of the population with a gain (log 2 = 0.2) or a loss (log 2 = -0.11) to correlate with the FISH cutoff of 30% (above). These values were either added or subtracted from the mean of the segments for each sample to generate a range of values, beyond which an event would simply be called a gain or loss. The number of probes scored as gain or loss was correlated to the matched FISH call for the same probes using Pearson's linear correlation. Limiting gains and losses to segments outside of 1 SD is similar to, but more stringent than, the thresholds recently used for significant segment detection in heterogeneous tumor samples (13). These formal FISH and aCGH comparisons are the only examples where log 2 thresholds are set at 30%; more stringent log 2 thresholds are set at 50% ($-0.192 < x > 0.319$) elsewhere in the article where CNAs are reported. All statistical comparisons were done using GraphPad InStat (version 3.06; GraphPad Software, Inc.) and $P \leq 0.05$ was considered significant.

## Results

***Detection of CNA by FISH.*** To determine gains and losses at individual loci, probe signals were matched to ploidy for each individual tumor: Five tumors were diploid, five were triploid, five were tetraploid, and the remaining four were $2n;3n$, $2n;4n$, $3n;6n$, and $3n;6n$, respectively. All 19 metastatic melanoma samples showed CNAs at loci associated with malignancy or at other critical cellular functions (Fig. 1). For instance, a large fraction of patient samples had copy number gains at *NEDD9* (6p24.1), *MET* (7q31), and *MYC* (8q24), and losses at *WISP3* (6q22), *CCND3* (6p21), *MLANA* (9p24.1), and *CDKN2A* (9p21). The changes were unidirectional at *CCND3*, *CDKN2A*, *ETS1* (11q24), and *APAF1* (12q23), but other probes showed some degree of both gain and loss, depending on the sample. Comparisons between gain or loss of loci on different chromosomes within the same sample or across samples were not possible within the available statistics. Many events involved large chromosomal regions, as evidenced by loss of signals on both arms of a particular chromosome, underscoring aneuploidy in cancer (14) and emphasizing a strength of aCGH analysis, where such large changes can be readily detected, over locus-specific FISH. *CDKN2A* was the only gene showing biallelic loss (in 3 of 13 samples) due to loss of either both chromosomes 9 (2 samples) or both 9p alleles, as implied by two coexisting signals from the *ABL1* FISH reference probe on 9q (data not shown). In samples where *NEDD9* and *WISP3* were used successfully in combination, 6 of 14 were opposite in sign (Fig. 1), suggesting coincident gains (6p) and losses (6q).

***Detection of CNA by aCGH.*** DNA was isolated from frozen touch-preparation slides and amplified for aCGH from 11 specimens where sample was available. The FISH pattern of CNAs across the set of probed genes for this sample subset ($n = 11$) was very similar to the overall pattern for all samples (data not shown). CNAs were initially visualized in Imagene as segments of change, which are at minimum three BACs in size due to the moving average that is used to determine regions of change (segments) along the genome (11). With increased

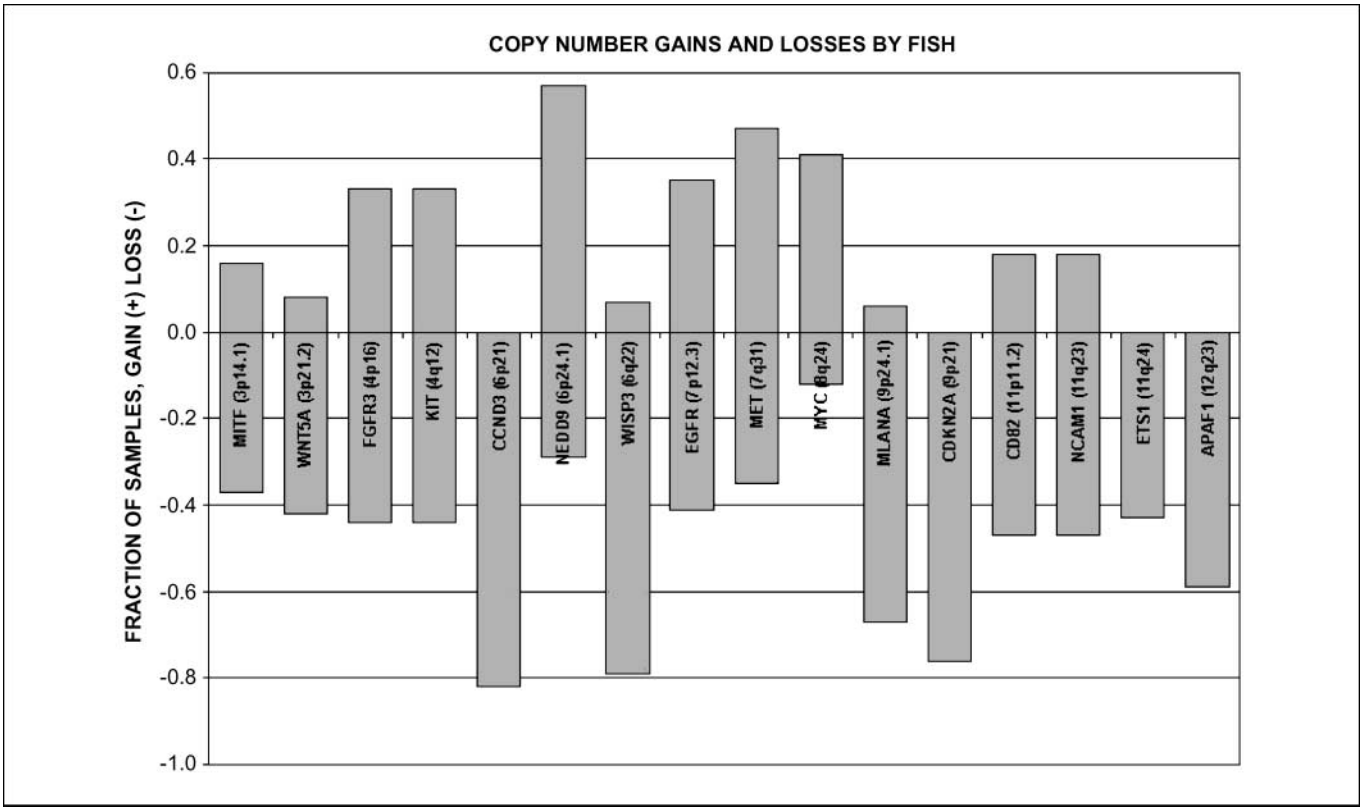


**Fig. 1.** Fractions of patient samples with CNAs detected by FISH. Gains and losses are plotted above (gain) or below (loss) the *x*-axis and the length of the bar represents the fraction of samples with a gain or loss (*y-axis*). FISH was done on 19 patient samples. Details of the criteria for calling a gain or loss are given in the text. The chromosome location of each probe and the locus identity are provided in Table 1.

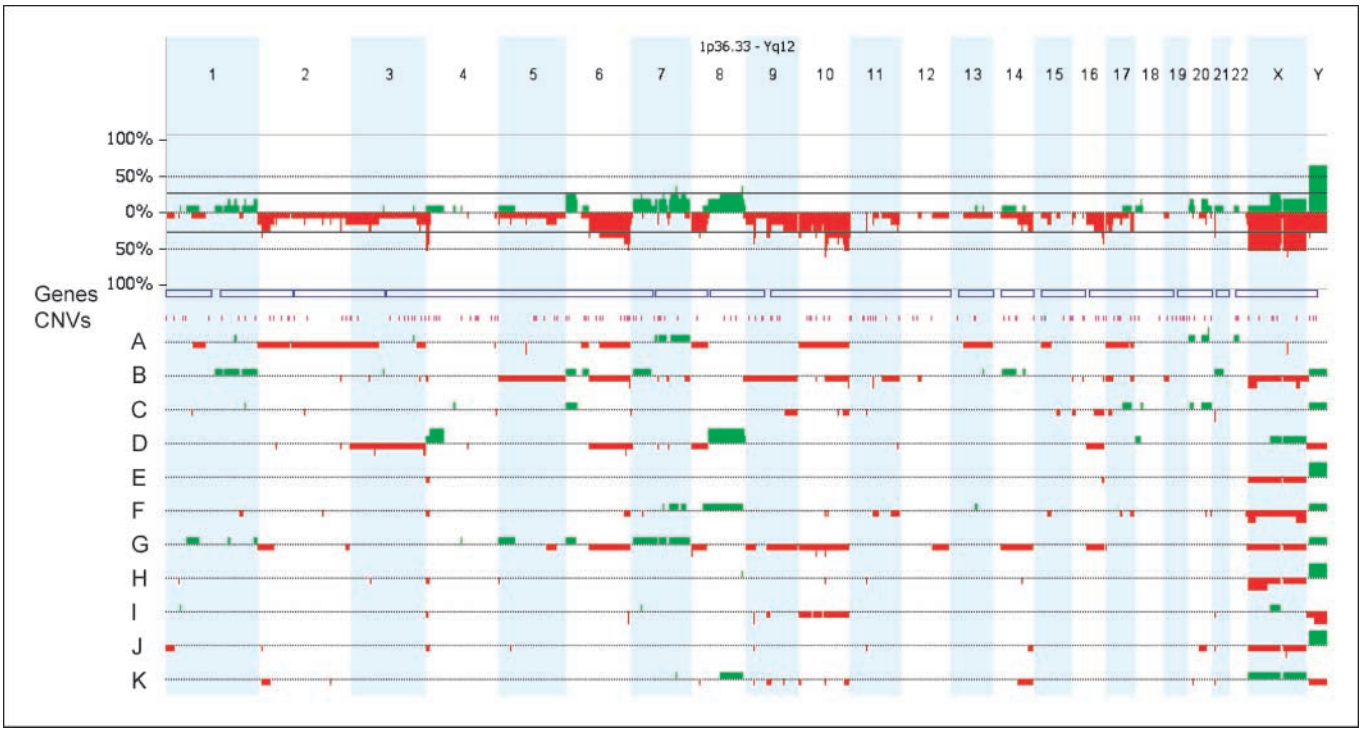


**Fig. 2.** CNAs across samples by aCGH. Aggregate CNA plots were developed using Nexus software (Biodiscovery). CNA was detected in all samples ($n$ = 11), which are plotted individually as indicated by a random letter along the left side of the figure. Any region that surpassed our threshold for gain or loss (-0.192 < $x$ > 0.319) is shown as a red (loss) or green (gain) segment of change. Chromosomes are plotted from left to right across the top and sized approximately to scale. The number of samples showing a particular change is plotted in the aggregate aCGH plot at the top, with the fraction of samples showing a segment change plotted numerically on the $y$-axis. Distinct local (e.g., chromosome 4p16) and regional (e.g., chromosome 6q) changes were frequent between samples. The individual sample plots show the aCGH data as either gain (+1) or loss (-1) on the $y$-axis, and the aggregate is frequency data on the $y$-axis; neither of these plots shows the actual log 2 ratios. Individual BAC log2 ratio values were compiled across samples and a mean was generated.

technical noise, the number of BAC elements required to define a segment increased. All of these segment changes met the thresholds for gain (0.319) and loss (-0.192) in each of the independent samples. The smallest individual uninterrupted segment was 0.223 Mb at 8p23.2, and the largest was 134.94 Mb and comprised the entire chromosome 10.

The aggregate aCGH profile generated in Nexus uncovered several common large (chromosome or arm) CNA regions: 6p, 8q, and chromosome 7 gains, and 6q, 8p, chromosome 9, 10, and 16 losses (Fig. 2), which agreed with the implied large-scale chromosome changes in our FISH data (Fig. 1) and support other cytogenetic evidence that large-scale chromosomal events are important in melanoma (6). For instance, almost half of the FISH-probed samples showed gain of *NEDD9* (6p) coincident with loss of *WISP3* (6q) (Figs. 1 and 2), which is also evident in the aCGH profiles shown in Figs. 2 and 3.

***Regions of CNA overlap.*** The aggregate aCGH profile built in Nexus generates an output that defines segments (regions) overlapping among samples that meet the set thresholds (e.g., -0.192 < $x$ > 0.319) and a specified frequency. The output frequency was set at 3 of 11 (27%) samples with a common segment gained or lost. Table 2 displays these changes, along with genes in the regions commonly associated with malignancy, based on publicly available interrogation databases: University of California Santa Cruz (15) and National Center for Biotechnology Information. Thirty-four segments were uncovered, including two involving exclusively the centromeric regions of chromosomes 6 and 9, which were discarded from Table 2 as likely aCGH artifact related to scarce BAC coverage at these regions, and one containing only normal CNV regions (12) but no genes (chromosome 8, Table 2). Segments of recurrent CNA included regions that were assessed in the FISH study spanning the genes *FGFR3*, *WNT5A*, *NEDD9*, *CDKN2A*, and *CD82* (Table 2). Most of the recurrent CNA segments were associated with larger-scale (chromosome or arm) events (e.g., chromosome 10 and chromosome 6p; Fig. 2; Table 2); a comprehensive set of candidate genes is not given for these larger regions in Table 2 due to space considerations. Many of these common segments were anticipated given the FISH data (Fig. 1) and the aggregate aCGH profile (Fig. 2). Other regions of recurrent CNAs that were not expressly investigated in the FISH study, but have been associated with malignancy, encompassed genes involved in TP53 pathways [i.e., *ZMIZ1* (PIAS-like protein; ref. 16) and *BANP* (splice variant of *SMAR1*; ref. 17)] and genes involved in DNA stability (*FANCA* and *XPA*).

***Comparison between aCGH and FISH.*** Individual BAC values for the panel of FISH probes were compared directly to the same set from the aCGH. This was done initially through visual inspection using the Imagene chromosome view pane for each probe and each sample. Figure 3 shows the concordance between FISH data and aCGH data for four different samples, four different chromosomes, and six different probes. Mathematical comparisons were also made. The aCGH data for each of the 11 samples were bracketed either by 1 SD from each sample mean or by log 2 values estimating 30% change (-0.11 < $x$ > 0.2), and the result was scored as either in agreement or not in agreement with the FISH data. Overall, both of these

bracketing approaches agreed well, and similarly, with the FISH data, with a high ratio of FISH calls to aCGH calls: 0.73 ± 0.062 SE and 0.72 ± 0.0739 SE, respectively, for 1 SD and log 2 bracketed data. The correlations between the 1 SD and 30% log 2 ratio bracketing approaches and the FISH data were significant ($r$ = 0.697, $P$ = 0.0172 and $r$ = 0.619, $P$ = 0.042, respectively).

## Discussion

We have described genome-wide CNA in a set of frozen touch-preparation slides from patients with metastatic melanoma using two techniques: FISH and aCGH. The correlations between the FISH and aCGH, while not unity, suggest that the methods are similar at detecting CNA at individual loci across a range of samples and sites. Furthermore, the loci for *FGFR3*, *WNT5A*, *NEDD9*, *CDKN2A*, and *CD82* all exist within aCGH segments (regions) of change and were also shown to have CNA by locus-specific FISH. That these loci exist on aCGH segments of change could permit rapid visual screening of aCGH results with fewer false negatives, which may streamline laboratory diagnostics. These data are similar to published reports of CNA in metastatic melanoma, by conventional cytogenetics (6), BAC aCGH (8), or single-nucleotide polymorphism aCGH (7), and support the notion that the above loci are important in

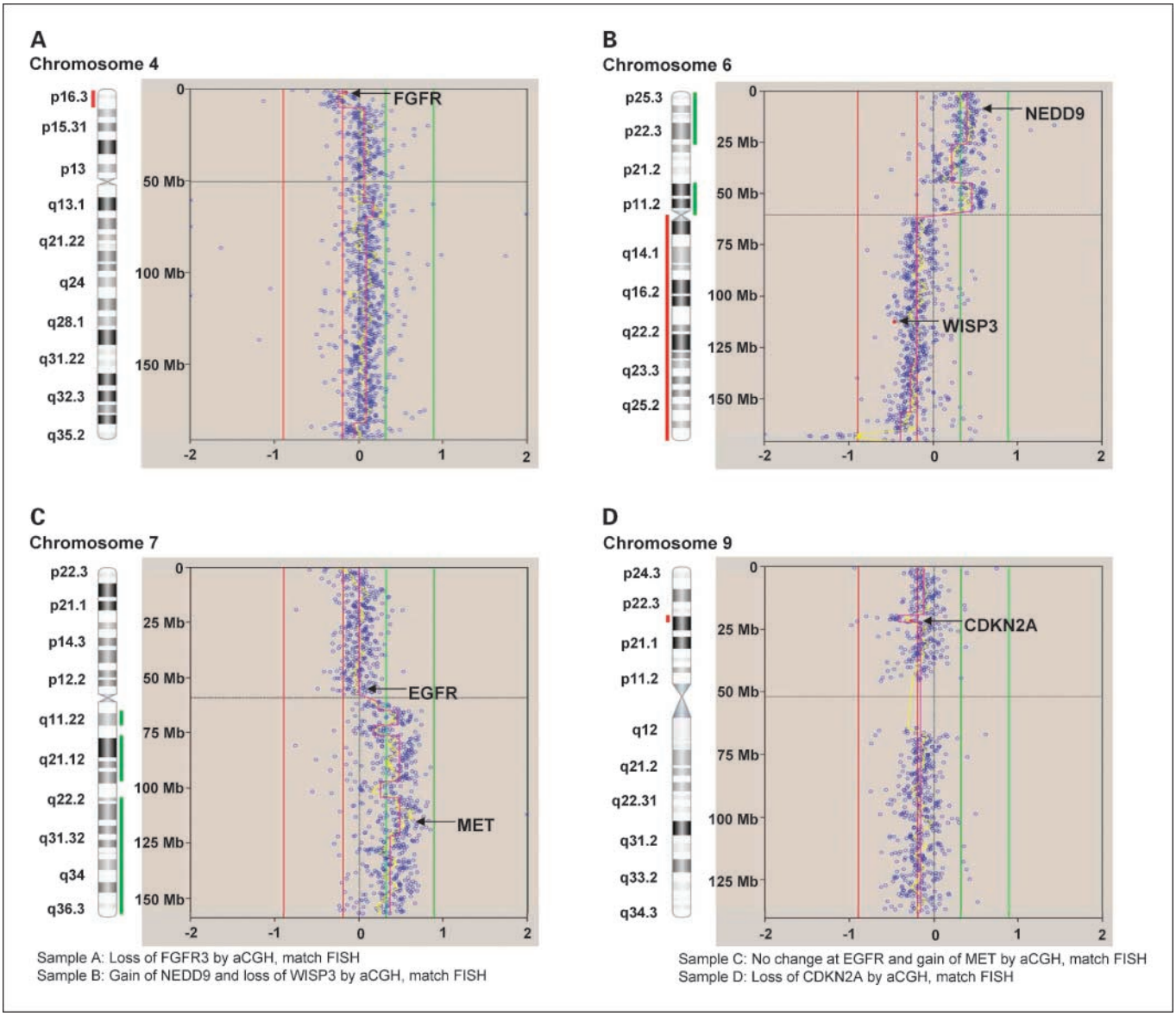


**Fig. 3.** Examples of concordance between FISH and aCGH. Several methods were used to determine concordance between FISH and aCGH copy number assessment and are detailed in the text. This figure provides a visual comparison using the Imagene software package (Biodiscovery) for four independent samples (from the same sample set used throughout, but classified here as 1-4). In this series of images, log 2 ratio is plotted on the $x$-axis and chromosomal location is on the $y$-axis, and as indicated by the ideogram. The midline represents a log 2 ratio of 0, where there is no change between tumor and control DNA. The first green (0.319) and red (-0.192) lines indicate single-copy gains and losses in 50% of the population; the outer green and red lines indicate two-copy gains and losses, respectively. The location of individual BACs spanning specific loci is indicated by an arrow. The outcome of aCGH (shown) and the FISH (data not shown) matched in each case. *A,* sample shows loss of *FGFR3*. *B,* sample shows a gain of *NEDD9* and loss of *WISP3*. *C,* sample shows no change at *EGFR* with gain of *MET*. *D,* sample shows loss of *CDKN2A*.

**Table 2.** Minimal regions of CNA observed across the malignant melanoma samples using aCGH

| Region | Region length | Cytoband | Event | Participation (%) | Gene* |
|---|---|---|---|---|---|
| chr2:8,029,505-10,673,929 | 2,644,424 | 2p25.1 | Deletion | 36.4 | *DDEF2, TAF1B, KLF11, ADAM17* |
| chr2:218,315,701-220,282,083 | 1,966,382 | 2q35 | Deletion | 27.3 | *TNS1, IL8RB, WNT6, WNT10A, CDK5R2* |
| chr3:49,222,550-50,741,118 | 1,518,568 | 3p21.3 | Deletion | 27.3 | *RASSFI, HYAL1, HYAL2, HYAL3, MAPKAPK3, TRAIP* |
| chr3:54,700,836-55,871,934 | 1,171,098 | 3p14.3 | Deletion | 27.3 | *WNT5A* |
| chr3:184,533,265-186,011,822 | 1,478,558 | 3q27 | Deletion | 27.3 | *DVL3, EPHB3, PSMD2* |
| chr4:752,619-8,384,706 | 7,632,087 | 4p16 | Deletion | 54.5 | *FGFR3, RGS12, MSX1, MXD4* |
| chr6:522,581-26,126,346 | 25,603,765 | 6p25.3-p22.2 | Gain | 27.3 | *NEDD9* |
| chr6:162,810,559-163,795,184 | 984,626 | 6q26 | Deletion | 54.5 | *PARK2, PACRG* |
| chr7:27,845,626-30,383,360 | 2,537,734 | 7p15.1 | Gain | 27.3 | *JAZF1, CHN2* |
| chr7:84,987,863-87,283,635 | 2,295,773 | 7q21.1 | Gain | 27.3 | *DMFT1, ABCB1* |
| chr7:118,941,035-124,625,514 | 5,684,479 | 7q31.31 | Gain | 36.4 | *ING3, WNT16, PTPRZ1, SPAM1, POT1* |
| chr7:131,765,107-146,524,565 | 14,759,459 | 7q32.3-q35 | Gain | 27.3 | *BRAF* |
| chr8:136,897,395-138,954,070 | 2,056,675 | 8q24.3 | Gain | 36.4 | All CNV (ref. 12) |
| chr8:22,415,074-23,500,458 | 1,085,385 | 8p21.3 | Deletion | 36.4 | *TNFRSF10A, TNFRSF10B, TNFRSF10C, TNFRSF10D* |
| chr9:21,391,626-22,461,995 | 1,070,369 | 9p21.3 | Deletion | 45.5 | *CDKN2A, CDKN2B* |
| chr9:97,924,515-99,826,848 | 1,902,333 | 9q22.3 | Deletion | 27.3 | *CDC14B, CTSL2, XPA* |
| chr9:103,917,197-138,169,393 | 34,252,196 | 9q31.1-q34.3 | Deletion | 27.3 | *TRAF1, ABL1, COL5A1* |
| chr10:214,399-8,254,557 | 8,040,158 | 10p15.3 | Deletion | 36.4 | *PRKCQ, NET1, KLF6, IL15RA, CALML5* |
| chr10:45,815,907-50,696,603 | 4,880,697 | 10q11.22 | Deletion | 36.4 | *GDF2, GDF10, PTPN20A, MAPK8* |
| chr10:70,657,572-73,408,999 | 2,751,427 | 10q22.1 | Deletion | 63.6 | *COL13A1* |
| chr10:78,124,861-81,012,814 | 2,887,953 | 10q22.3 | Deletion | 45.5 | *DLG5, POLR3A, ZMIZ1* |
| chr10:104,807,274-106,164,190 | 1,356,916 | 10q24.33 | Deletion | 45.5 | *COL17A1, CLK, GSTO1* |
| chr10:120,589,963-135,279,389 | 14,689,426 | 10q26.11-q26.3 | Deletion | 54.5 | Region of frequent deletions in cancer |
| chr11:43,746,558-45,742,554 | 1,995,996 | 11p11.2 | Deletion | 27.3 | *CD82* |
| chr11:125,755,500-126,840,169 | 1,084,669 | 11q24.2 | Deletion | 27.3 | *ETS1* †, *CHEK1* † |
| chr14:75,508,420-76,734,126 | 1,225,706 | 14q24.3 | Deletion | 27.3 | *TGFB3* |
| chr14:90,510,546-105,306,795 | 14,796,249 | 14q32.12-q32.33 | Deletion | 27.3 | *TRAF3* |
| chr16:82,212,240-88,637,968 | 6,425,729 | 16q23.3q24.3 | Deletion | 45.5 | *BANP, CBFA2T3, FANCA, CDK10* |
| chr17:373,081-5,206,982 | 4,833,901 | 17p13.3 | Deletion | 27.3 | *MNT* |
| chr17:7,436,435-20,113,657 | 12,677,222 | 17p13.1-p11.2 | Deletion | 27.3 | *TP53, TNFRSF13B* |
| chr17:68,018,598-78,206,787 | 10,188,189 | 17q24.3-q25.3 | Deletion | 27.3 | *CDK3, FB1, ITGB4, C1QTNF1* |
| chr21:9,954,111-11,742,879 | 1,788,768 | 21p11.2 | Deletion | 36.4 | *TPTE, BAGE2, BAGE3, BAGE4, BAGE5* |

*HUGO nomenclature.
†These genes, assessed in the FISH study, are very near the CNA listed here, 1 Mb for *ETS1* and 0.6 Mb for *CHEK1*.

melanoma metastasis and may provide valuable markers for metastasis generally.

A strength of the current study is that actively dividing cells were not required for the assays done and thus there was no potential for selective pressure during *in vitro* propagation. This may also affect the data in that inactive, dead, and dying cells are assessed, which would not be anticipated to contribute to the molecular signature *in vitro*. Overall, our data are very similar to a recent melanoma genomic profiling report using a similar BAC-based aCGH platform (18), but differences may speak to the fact that the current study assessed CNA in metastatic lesions prepared directly from patient biopsy material whereas Jonsson et al. (18) used malignant melanoma cell lines. That the two studies produced overlapping CNA data, however, bolsters the notion that a common set of chromosomal alterations may define malignant melanoma: CNA gains at chromosomes 7p, 7q, and 8q and losses at 4p, 6q, 8p, 9p, 10, and 11q (Table 2; ref. 18).

A clear biological role in melanoma metastasis has been determined for loss of *CDKN2A* (19–21), *WNT5A* (22) and gain of *NEDD9* (23), all of which are readily detected using techniques described in the current article. However, the contribution of FGFR3 and *CD82* to melanoma metastasis may largely be mediated indirectly through downstream effectors of FGFR3, such as members of the Ras/Raf/mitogen-activated protein kinase pathway (24), which may be regulated by *BRAF* (25). Down-regulation of *CD82* is observed in the advanced stages of a wide variety of cancers including skin (26). In addition, the CNA regions including the *FGFR3* and *CD82* loci contain other genes. For instance, the ~2-Mb region on chromosome 11q including *CD82* spans the locus for a TP53-induced protein (TP53I11). The 7.5-Mb region including *FGFR3* also includes loci for RGS12, a member of a family of proteins that regulates G protein signaling, the MSH homeobox gene *MSX1*, and the MAD protein family gene *MXD4*. Collectively, these studies may aid in the synthesis of pathways and in the determination of the point of convergence for the general pathway or pathways disrupted in malignant melanoma, which may guide targeted therapy (27, 28). However, it will be important to extend these studies to include nonmetastatic samples.

Several explanations may underlie the lack of complete concordance between the FISH and aCGH data in detecting CNA. For instance, the locus for *FGFR3* was observed as a gain and loss roughly equally by FISH (Fig. 1), but as a loss in 50% and a gain in 15% of samples by aCGH (Fig. 2). Mathematically, 30% of a 3*n* population with single-copy gain (to 4*n* total) would be scored by FISH as a gain; by aCGH, the same region in the same population would require 1.5 extra copies to be scored as a gain. Similarly, 30% of a 3*n* population with 2

extra copies (to 5*n* total) would simply be counted as a gain by FISH, whereas the same event would be counted as more than a gain by aCGH. Technically, it is possible that a small number of micronuclei and apoptotic cells, or adjacent, nontarget cell populations, were excluded in the FISH analysis, which could contribute to the whole extracted DNA in aCGH analyses, particularly when microdissection is not done (9). It is also possible that the whole genome amplification used before aCGH resulted in allele bias. However, we feel that this is unlikely because it has recently been reported, using the same amplification protocol, that as few as 100 isolated and amplified cells were sufficient to simulate the aCGH profile of an unamplified control population accurately (9). Furthermore, as outlined in Table 1, due to limitations of probe availability at study inception and limited clinical sample, some of the FISH probes did not encompass the genomic locus, but mapped nearby. A probe prepared from the BAC RP11-154H23 was used to detect changes in MITF, but was 1.5 Mb centromeric. In addition, some probes were not included as part of the RPCI aCGH array or did not hybridize successfully on the array. Despite these limitations, a set of loci was identified as positive by FISH and as positive by aCGH, both as individual elements of change and as components of a segment of change (above).

A major advantage of aCGH over locus-specific FISH in detection of CNA is the ability to interrogate the whole genome in a single assay, which makes it a powerful discovery tool. On the other hand, changes in individual elements require a high degree of scrutiny; they may be particularly difficult to detect as they may be associated with a segment that is opposite in sign or does not reach a detection threshold. Other changes may result from translocations or microdeletions. For example, aberrant NOTCH1 (9q34.3) expression and signaling has been reported in metastatic melanoma (29), in addition to myriad other malignancies (30). In the current experiments, the mean *NOTCH1* log 2 value (RP11-707O3) was -0.27 ($\pm$0.059 SE), suggesting that a larger fraction of the population of samples (68%) had lost a copy of *NOTCH1* than would be estimated from the general overall trend across samples toward chromosome 9 loss by examination of aCGH segments. In addition, although the current aCGH experiments detected the region including *BRAF* as a CNA region (Table 2), *BRAF* mutations could not have been detected, which are common in melanoma (25, 28).

Gene CNAs in melanoma may have clinical utility in several respects. First, specific patterns of deletions and/or gains may be associated with different outcomes in patients with stage IV metastatic resected disease (the cohort for this study). We already know that these patients can have extremely different survival outcomes, although all are resected to be free of disease. Second, CNA detection by FISH may provide better guidelines for selecting patients for surgical therapy. In the future, we hope to apply CNA techniques to a larger group of patients with resected stage IV melanoma, as well as patients with (macroscopic) stage IIIB/C melanoma, to determine whether specific CNA are associated with metastases to certain organ sites and/or better or worse outcomes after resection. Third, perhaps the most important contribution of CNA technology may be increased ability to characterize and select patients being considered for "molecularly targeted" therapy in early stages of disease. We have previously shown that CNA may be detected by aCGH technology using paraffin-embedded or frozen tissue samples enriched for tumor cells (9). Single gene mutations are of limited significance because loss or gain of other genes may influence the response of a tumor to a specific inhibitor of the mutated target protein. In the clinic, agents are already available that target *MET*, *EGFR*, and *KIT*, and histone deacetylating agents may enhance expression of *APAF1*. Based on the promising preliminary results of this study, CNA detection should be incorporated into future therapeutic trials using these new agents. Furthermore, CNA correlation with response to therapy and other clinical pathologic correlates in these trials should allow us to move personalized "targeted" therapy forward in malignant melanoma and to define those patients who are most likely to benefit.

In summary, we present an analysis of CNAs in metastatic melanoma using two distinct but complementary cytogenetic approaches: locus-specific FISH and aCGH. Both performed well on touch preparations that had been frozen and gave similar results in pairwise comparisons at individual loci. Several recurrent CNAs, from the chromosomal scale to the level of individual loci, were detected, many of which resided on aCGH segments of change, which are statistically relevant and relatively easy to detect on visual examination of individual or composite aCGH profiles. Incorporation of correlated gene expression profiles into CNA findings similar to those from this study may provide more specific areas for investigation for future studies examining genetic markers that are critical in malignant melanoma and possibly relevant to metastasis of other tumor types.

## Disclosure of Potential Conflicts of Interest

J. Sosman has commercial research grants from Genentech, Astra Zeneca, and Medarax. V. Sondak is or has served as a consultant for Schering-Plough, Pfizer, BMS/Medarax, Bayer/Onyx, Glaxo, and Smith-Kline/Synta.

## References


1. Jemal A, Siegel R, Ward E, et al. Cancer statistics. CA Cancer J Clin 2008;58:71–96.
2. Lewis TB, Robison JE, Bastien R, et al. Molecular classification of melanoma using real-time quantitative reverse transcriptase-polymerase chain reaction. Cancer 2005;104:1678–86.
3. Chin L, Garraway LA, Fisher DE. Malignant melanoma: genetics and therapeutics in the genomic era. Genes Dev 2006;20:2149–82.
4. Casorzo L, Luzzi C, Nardacchione A, Picciotto F, Pisacane A, Risio M. Fluorescence *in situ* hybridization (FISH) evaluation of chromosomes 6, 7, 9 and 10 throughout human melanocytic tumorigenesis. Melanoma Res 2005;15:155–60.
5. Glatz-Krieger K, Pache M, Tapia C, et al. Anatomic site-specific patterns of gene copy number gains in skin, mucosal, and uveal melanomas detected by fluorescence *in situ* hybridization. Virchows Arch 2006;449:328–33.
6. Hoglund M, Gisselsson D, Hansen GB, et al. Dissecting karyotypic patterns in malignant melanomas: temporal clustering of losses and gains in melanoma karyotypic evolution. Int J Cancer 2004;108:57–65.
7. Stark M, Hayward N. Genome-wide loss of heterozygosity and copy number analysis in melanoma using high-density single-nucleotide polymorphism arrays. Cancer Res 2007;67:2632–42.
8. Jonsson G, Dahl C, Staaf J, et al. Genomic profiling of malignant melanoma using tiling-resolution array CGH. Oncogene 2007;108:57–65.
9. Nowak NJ, Miecznikowski J, Moore SR, et al. Challenges in array CGH for the analysis of cancer samples. Genet Med 2007;9:585–95.
10. Cowell JK, Nowak NJ. High-resolution analysis of genetic events in cancer cells using bacterial artificial chromosome arrays and comparative genome hybridization. Adv Cancer Res 2003;90:91–125.

**11.** Olshen AB, Venkatraman ES, Lucito R, Wigler M. Circular binary segmentation for the analysis of array-based DNA copy number data. Biostatistics 2004;5:557–72.

**12.** Redon R, Ishikawa S, Fitch KR, et al. Global variation in copy number in the human genome. Nature 2006;444:444–54.

**13.** Fiegler H, Geigl JB, Langer S, et al. High resolution array-CGH analysis of single cells. Nucleic Acids Res 2007;35:e15.

**14.** Duesberg P, Li R, Fabarius A, Hehlmann R. The chromosomal basis of cancer. Cell Oncol 2005;27:293–318.

**15.** Kent WJ, Sugnet CW, Furey TS, et al. The human genome browser at UCSC. Genome Res 2002;12:996–1006.

**16.** Lee J, Beliakoff J, Sun Z. The novel PIAS-like protein hZimp10 is a transcriptional co-activator of the p53 tumor suppressor. Nucleic Acids Res 2007;35:4523–34.

**17.** Kaul R, Mukherjee S, Ahmed F, et al. Direct interaction with and activation of p53 by SMAR1 retards cell-cycle progression at $G_2$/M phase and delays tumor growth in mice. Int J Cancer 2003;103:606–15.

**18.** Jönsson G, Dahl C, Staaf J, et al. Genomic profiling of malignant melanoma using tiling-resolution array-CGH. Oncogene 2007;26:4738–48.

**19.** Walker GJ, Flores JF, Glendening JM, Lin AH, Markl ID, Fountain JW. Virtually 100% of melanoma cell lines harbor alterations at the DNA level within CDKN2A, CDKN2B, or one of their downstream targets. Genes Chromosomes Cancer 1998;22:157–63.

**20.** Puig S, Castro J, Ventura PJ, et al. Large deletions of chromosome 9p in cutaneous malignant melanoma identify patients with a high risk of developing metastases. Melanoma Res 2000;10:231–6.

**21.** Fargnoli MC, Argenziano G, Zalaudek I, Peris K. High- and low-penetrance cutaneous melanoma susceptibility genes. Expert Rev Anticancer Ther 2006;6:657–70.

**22.** Dissanayake SK, Wade M, Johnson CE, et al. The Wnt5A/protein kinase C pathway mediates motility in melanoma cells via the inhibition of metastasis suppressors and initiation of an epithelial to mesenchymal transition. J Biol Chem 2007;282:17259–71.

**23.** Kim M, Gans JD, Nogueira C, et al. Comparative oncogenomics identifies NEDD9 as a melanoma metastasis gene. Cell 2006;125:1269–81.

**24.** Cheng SL, Huang-Liu R, Sheu JN, Chen ST, Sinchaikul S, Tsay GJ. Toxicogenomics of A375 human malignant melanoma cells. Pharmacogenomics 2007;8:1017–36.

**25.** Davies H, Bignell GR, Cox C, et al. Mutations of the BRAF gene in human cancer. Nature 2002;417:949–54.

**26.** Tonoli H, Barrett JC. CD82 metastasis suppressor gene: a potential target for new therapeutics? Trends Mol Med 2005;11:563–70.

**27.** Gray-Schopfer V, Wellbrock C, Marais R. Melanoma biology and new targeted therapy. Nature 2007;445:851–7.

**28.** Sosman JA, Puzanov I. Molecular targets in melanoma from angiogenesis to apoptosis. Clin Cancer Res 2006;12:2376–83s.

**29.** Haass NK, Herlyn M. Normal human melanocyte homeostasis as a paradigm for understanding melanoma. J Investig Dermatol Symp Proc 2005;10:153–63.

**30.** Shih IeM, Wang TL. Notch signaling, γ-secretase inhibitors, and cancer therapy. Cancer Res 2007;67:1879–82.

**31.** Garraway LA, Widlund HR, Rubin MA, et al. Integrative genomic analyses identify MITF as a lineage survival oncogene amplified in malignant melanoma. Nature 2005;436:117–22.

**32.** McGill GG, Horstmann M, Widlund HR, et al. BCL2 regulation by the melanocyte master regulator Mitf modulates lineage survival and melanoma cell viability. Cell 2002;109:707–18.

**33.** Du J, Miller AJ, Widlund HR, Horstmann MA, Ramaswamy S, Fisher DE. MLANA/MART1 and SILV/PMEL17/GP100 are transcriptionally regulated by MITF in melanocytes and melanoma. Am J Pathol 2003;163:333–43.

**34.** Weeraratna AT, Jiang Y, Hostetter G, et al. Wnt5a signaling directly affects cell motility and invasion of metastatic melanoma. Cancer Cell 2002;1:279–88.

**35.** Trudel S, Stewart AK, Rom E, et al. The inhibitory anti-FGFR3 antibody, PRO-001, is cytotoxic to t(4;14) multiple myeloma cells. Blood 2006;107:4039–46.

**36.** Potti A, Ganti AK, Foster H, et al. Immunohistochemical detection of HER-2/neu, c-kit (CD117) and vascular endothelial growth factor (VEGF) overexpression in soft tissue sarcomas. Anticancer Res 2004;24:333–7.

**37.** Spofford LS, Abel EV, Boisvert-Adamo K, Aplin AE. Cyclin D3 expression in melanoma cells is regulated by adhesion-dependent phosphatidylinositol 3-kinase signaling and contributes to $G_1$-S progression. J Biol Chem 2006;281:25644–51.

**38.** Florenes VA, Faye RS, Maelandsmo GM, Nesland JM, Holm R. Levels of cyclin D1 and D3 in malignant melanoma: deregulated cyclin D3 expression is associated with poor clinical outcome in superficial melanoma. Clin Cancer Res 2000;6:3614–20.

**39.** Kleer CG, Zhang Y, Pan Q, et al. WISP3 and RhoC guanosine triphosphatase cooperate in the development of inflammatory breast cancer. Breast Cancer Res 2004;6:110–5.

**40.** Zhang Y, Pan Q, Zhong H, Merajver SD, Kleer CG. Inhibition of CCN6 (WISP3) expression promotes neoplastic progression and enhances the effects of insulin-like growth factor-1 on breast epithelial cells. Breast Cancer Res 2005;7:1080–9.

**41.** Clark EA, Golub TR, Lander ES, Hynes RO. Genomic analysis of metastasis reveals an essential role for RhoC. Nature 2000;406:532–5.

**42.** Nelson MA, Radmacher MD, Simon R, et al. Chromosome abnormalities in malignant melanoma: clinical significance of nonrandom chromosome abnormalities in 206 cases. Cancer Genet Cytogenet 2000;122:101–9.

**43.** Boccaccio C, Comoglio PM. Invasive growth: a MET-driven genetic programme for cancer and stem cells. Nat Rev Cancer 2006;6:637–45.

**44.** Koynova D, Jordanova E, Kukutsch N, van der Velden P, Toncheva D, Gruis N. Increased C-MYC copy numbers on the background of CDKN2A loss is associated with improved survival in nodular melanoma. J Cancer Res Clin Oncol 2007;133:117–23.

**45.** Busam KJ, Jungbluth AA. Melan-A, a new melanocytic differentiation marker. Adv Anat Pathol 1999;6:12–8.

**46.** Talantov D, Mazumder A, Yu JX, et al. Novel genes associated with malignant melanoma but not benign melanocytic lesions. Clin Cancer Res 2005;11:7234–42.

**47.** Takaoka A, Hinoda Y, Sato S, et al. Reduced invasive and metastatic potentials of KAI1-transfected melanoma cells. Jpn J Cancer Res 1998;89:397–404.

**48.** Goldberg EK, Glendening JM, Karanjawala Z, et al. Localization of multiple melanoma tumor-suppressor genes on chromosome 11 by use of homozygosity mapping-of-deletion analysis. Am J Hum Genet 2000;67:417–31.

**49.** Rothhammer T, Poser I, Soncin F, Bataille F, Moser M, Bosserhoff AK. Bone morphogenic proteins are overexpressed in malignant melanoma and promote cell invasion and migration. Cancer Res 2005;65:448–56.

**50.** Torlakovic EE, Bilalovic N, Nesland JM, Torlakovic G, Florenes VA. Ets-1 transcription factor is widely expressed in benign and malignant melanocytes and its expression has no significant association with prognosis. Mod Pathol 2004;17:1400–6.

**51.** Fujimoto A, Takeuchi H, Taback B, et al. Allelic imbalance of 12q22-23 associated with APAF-1 locus correlates with poor disease outcome in cutaneous melanoma. Cancer Res 2004;64:2245–50.

**52.** Niedojadlo K, Labedzka K, Lada E, Milewska A, Chwirot BW. Apaf-1 expression in human cutaneous melanoma progression and in pigmented nevi. Pigment Cell Res 2006;19:43–50.